

Photoswitches in Order: One-Pot Synthesis of Azobenzene Main-Chain and Segmented Copolymers

Ruggero Rossi, Daniele Martella,* Camilla Parmeggiani, Max Hirschmann,* and Tiziana Fuoco

Cite This: *ACS Appl. Polym. Mater.* 2024, 6, 1563–1572

Read Online

ACCESS |

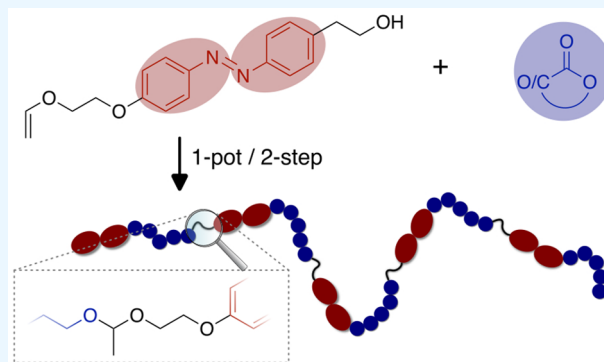
Metrics & More

Article Recommendations

Supporting Information

ABSTRACT: Syntheses of multifunctional polymers aim to engineer a wide range of material properties by adjusting the composition and positioning of functional groups. While manifold syntheses of side-chain-functionalized polymers are known, synthetic protocols for main-chain-functionalized polymers are less common. This work describes a general one-pot strategy to prepare polymers containing multiple functional moieties in their main-chain, e.g., azobenzene units separated by variable oligomers. The polymerization proceeds in two steps, starting from a single azobenzene initiator and commercially available monomers (lactones and cyclic carbonates). Various main-chain-functionalized polymers were obtained with a predictable and adjustable ratio of monomer units (5–20) to photoswitchable azobenzene groups. The thermal properties of these polymers were analyzed and rationalized with regard to the parent polymers' properties and the peculiarities arising from their segmented microstructure. Furthermore, the azobenzenes' ability to undergo light-induced *cis/trans*-isomerization is confirmed. High isomerization yields of up to 90% were observed for the polymers in solution with a half-life of several days for the *cis*-isomers in solution. When irradiated as solid films, the azobenzenes still undergo isomerization, but the *cis*-isomers are less stable compared to the liquid state.

KEYWORDS: azobenzene, mainchain, polyester, polycarbonate, photoisomerism, photoswitch



1. INTRODUCTION

Polymers bearing multiple functional groups promise extra functionality and tuneable properties imposed by their microstructures.^{1,2} However, while polymerizations of different side-chain-functionalized monomers and postpolymerization modifications to obtain (random) copolymers are common,^{3–5} a modular synthesis of copolymers with multiple main-chain functional groups is often more complex. Recently, some of us published a synthetic strategy that combined anionic ring-opening polymerization (ROP) and step-growth polymerization (SGP) in a two-step/one-pot manner,⁶ allowing one to alternate acetal functional groups with oligomers of polyesters (or polycarbonates). By changing the oligomers' length, the relative amount and spacing of acetal groups in the main-chain were controlled, which greatly influenced the polymer properties such as its degradation rate in specific conditions.

Moving toward a general procedure to introduce stimuli-responsive groups into the main-chain, we aimed to understand if this methodology could be adapted for the incorporation of moieties that react to one or multiple external influences in a designed and predictable manner. Such polymers are also referred to as stimuli-responsive or smart polymers and find manifold applications,⁷ e.g., in biomedicine⁸ or as molecular machines.⁹ Among the different external

stimuli, light is of particular interest because it is noninvasive, tuneable by its wavelength, and applicable with spatial and temporal control.¹⁰ If the reaction to the light stimulus is further reversible (e.g., by applying light of another wavelength or by thermal relaxation), the corresponding light-responsive moiety is called photoswitch and can trigger a reversible response of the polymer when inserted in their structure.¹¹ These reversible responses are again manifold, ranging from dissolved polymers that change their conformation and thereby the solution properties,^{12,13} to the control of inter- and intramolecular forces¹⁴ or solid–liquid^{15,16} and solid–liquid crystalline^{17,18} phase transitions of the polymer systems, respectively.

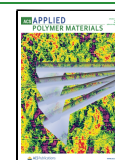
Incorporation of photoswitches into the polymer is possible either in the side-chains or in the main-chain of the polymer (cf., Scheme 1a). Within the main-chain, the photoswitch can be introduced as the initiator or end-capping species, whereby

Received: November 21, 2023

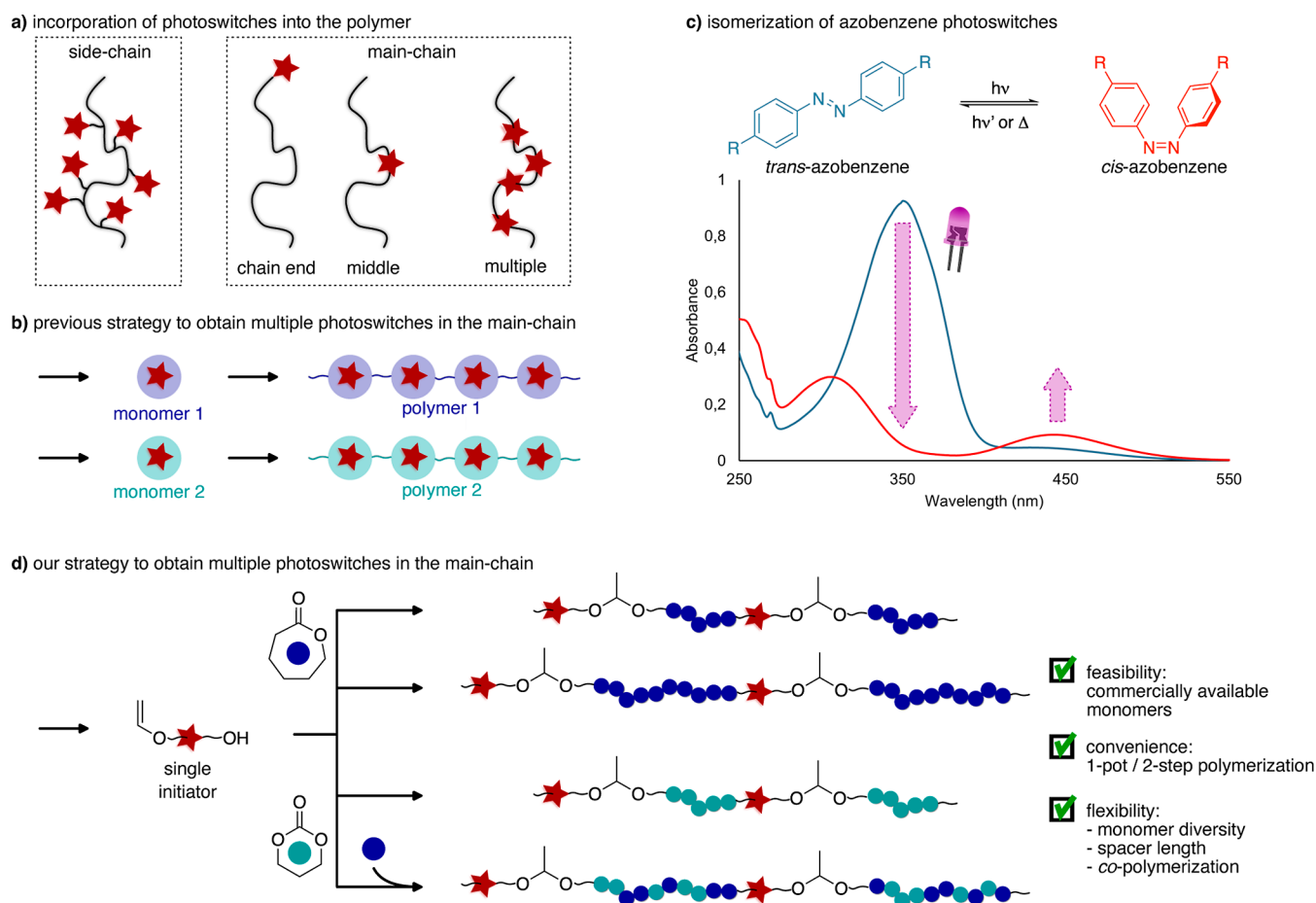
Revised: December 23, 2023

Accepted: December 26, 2023

Published: January 11, 2024



Scheme 1. Concept of the Work: (a) Different Ways to Covalently Bond Photoswitches to a Polymer Chain, (b) Previous Approaches to Synthesize Polymers with Multiple Photoswitches in the Main-Chain that Require Individual Monomer Syntheses to Obtain Different Polymers, (c) Change in the Molecular Conformation (Top) and Light Absorption Spectra of the Two Isomers (the Photoisomerization Process is Reversible by Irradiation with Different Wavelengths) and (d) Our Approach to Synthesize a Variety of Main-Chain-Functionalized Polymers from a Single Photoswitch-Containing Initiator and Commercially Available Monomers



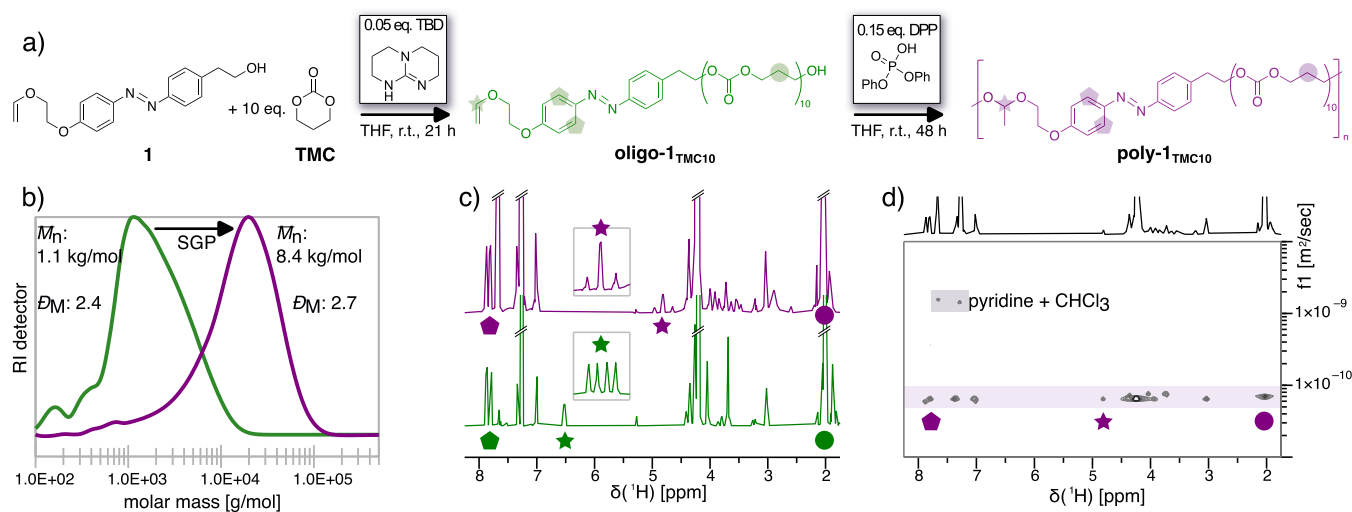
a single photoswitch ends up at the chain end or in the middle of the polymer/junction of a block copolymer. Multiple incorporation of photoswitches into the main-chain is, however, less frequent as it often requires a multistep synthesis of polymerizable photoswitches that are subsequently converted into polymers by, e.g., controlled radical,¹⁹ metathesis,^{20–23} condensation,^{24–27} addition,^{28–31} and click-reaction¹⁶ polymerization techniques. The common drawback of these strategies is that each polymer requires the synthesis of a unique monomer, which includes the establishment of—customized—purification procedures capable to achieve high monomer purity (cf. Scheme 1b).

Although being synthetically more challenging, incorporation of photoswitches directly into the main-chain of a polymer is desirable, as it promises a more direct and potentially stronger response of the polymer to the light stimulus. The most frequent used photoswitches in that regard—despite the large number of known photoswitches³²—are azobenzenes.³³ Their two conformations, the *trans*-state with the two phenyl rings being planar, and the *cis*-state with twisted phenyl rings and increased dipole moment, are interconvertible by light. The change in optical properties of an unsubstituted azobenzene under irradiation with UV light is shown in Scheme 1c, and such photoisomerizations were used to control

many properties in the materials where they are dispersed, e.g., their shape,³⁴ wettability,³⁵ and adhesion to other materials.³⁶ After a sufficient irradiation time (i.e., in equilibrium), the ratio of both states depends on many factors, including the light's wavelength and intensity. For the unsubstituted azobenzene, exposure to ultraviolet (UV) light leads to a photostationary state (ps) majorly consisting of the *cis*-species, and exposure to visible light or heat recovers a state majorly consisting of the *trans*-species. When incorporated into a polymer's main-chain, the azobenzene's *trans/cis*-isomerization changes the local constraints within the polymer backbone (geometry change of the azobenzene) and the ability to interact with other azobenzenes (both intra- and intermolecularly) through π - π stacking only possible for the *trans*-species.³⁷

Aside from the photoswitch, the light-induced isomerization also depends on the nature of the polymer (monomer structure) and its microstructure (e.g., the distance between the photoswitches in the backbone). These parameters control the local environment of the photoswitches and influence its isomerization behavior through so-called matrix effects.^{38,39} The limited free volume and the reduced segmental motion of the polymer usually lower the isomerization tendency as compared to the photoswitch in solution. On the other hand, as these parameters are imposed by the polymer, they are

Scheme 2. Synthesis of Poly-[AB-acetal-(TMC₁₀)] (Poly-1_{TMC10}, in Purple) from Azobenzene Initiator 1 and TMC via Macromonomer Oligo-1_{TMC10} (in Green) (a). Polymerization of the Macromonomer Leads to an Increased Molar Mass (Observed by SEC) (b) and to the Disappearance of the ¹H NMR Signals of the Vinyl Bond (c). ¹H NMR Signals Corresponding to the Azobenzene and TMC Units Have a Single Diffusion Coefficient (Observed by ¹H DOSY NMR) (d), Indicating that They Belong to the Same Polymer



controllable by choosing a polymer with suitable properties (e.g., by adjusting the glass-transition temperature T_g of the polymer). The easiest way to control and predict such polymer properties would be to rely on commodity polymers⁴⁰ and to regularly insert photoswitches into their main-chain, instead of synthesizing new monomers that yield polymers with unknown properties.

Regarding the synthesis of polymers with photoswitches incorporated into their main-chain, a procedure that (i) enables the polymerization of a variety of commercially available monomers, (ii) is easy to perform, and (iii) achieves control of the obtained microstructure is desirable. We hypothesized that combined anionic ROP and SGP in a two-step/one-pot manner, as previously described,⁶ yields azobenzene main-chain polymers and meets the three desired characteristics: (i) the polymerization of commercially available lactones and cyclic carbonates, (ii) in one-pot at room temperature, and (iii) with distance-control of photoswitches by adjusting the ratio of initiator to monomers (cf. Scheme 1d).

Herein, we present the results of the synthesis of an azobenzene initiator and its successful use to access main-chain-functionalized polyesters and polycarbonates with controllable azobenzene-spacing along the polymer backbones. The effect of the precise incorporation of azobenzene units into the main-chain on the thermal behavior is quantified and compared with the parent (unmodified) polymers. Finally, the photoisomerization and half-life are explored for the polymers in solution and as solid films. The one-pot synthetic strategy described opens the way for the easy preparation of a wide range of polymers with repeating sequential functional groups in the main-chain, where the specific functional moiety (demonstrated here for the azobenzene but easily extendable to many other moieties) is inserted between oligomeric blocks composed by arbitrary monomers and polymerization degree.

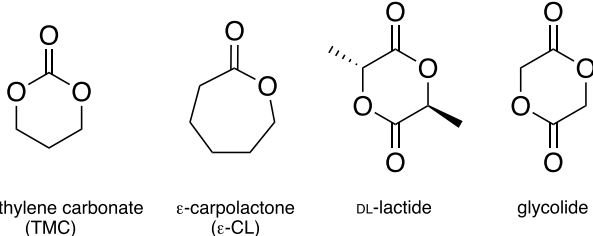
2. RESULTS AND DISCUSSION

2.1. Synthesis of Main-Chain-Functionalized Polymers. Azobenzene 1 was used as the initiator for all

polymerizations, and it was synthesized in two steps from commercially available precursors in 75% overall yield (cf. Supporting Information, p. SI-4ff. for further details). In particular, the multifunctional initiator 1 has been prepared by formation of the diazonium salt from 2-(4-aminophenyl)-ethanol and its coupling with phenolate as nucleophile to form the azobenzene core, followed by a Williamson reaction with 2-chloroethyl vinyl ether to introduce the final vinyl moiety. The preparation of different main-chain-functionalized polymers followed the procedure described in detail for the polymerization of trimethylene carbonate (TMC) as an example in Scheme 2a (cf. Supporting Information, p. SI-8ff. for further details). As already mentioned, a main-chain-functionalized polymer was obtained exploiting both reactive groups presented on the azobenzene initiator only by switching of the reaction catalyst in a one-pot procedure.⁶ More in details, the hydroxyl group was employed to start a ROP with triazabicyclodecene (TBD) base as the catalyst. Later, the vinyl group reacted with the terminal hydroxyl of the just prepared oligomers to form acetal bonds in a SGP catalyzed by diphenyl phosphate (DPP) acid.

The ROP yields oligomer **oligo-1_{TMC10}**, where TMC₁₀ refers to a 10-fold excess of TMC units with respect to the azobenzene initiator. After full conversion of TMC (as monitored by ¹H NMR), **oligo-1_{TMC10}** is obtained with a number-average molar mass \overline{M}_n of 1.1 kg/mol and its vinyl ether end group still intact, as evidenced by the ¹H NMR signal at 6.5 ppm with the characteristic fine structure (cf. Scheme 2c).

In the second step, a three-fold excess of DPP acid with respect to TBD is added to the reaction mixture, which initiates SGP. Under these acidic conditions, intermolecular addition of the oligomer's complementary alcohol and vinyl ether end groups occurs yielding acetal groups and, thus, growing the polymer chain. The disappearance of the ¹H NMR signals corresponding to the vinyl ether group and the appearance of characteristic acetal signals below 5 ppm together with an increased molar mass \overline{M}_n of 8.4 kg/mol (cf.

Table 1. Composition and Molar Mass Distributions of the Synthesized Polymers^a


#	monomers		feed ^b		X ^c		oligomer			polymer		
	1	2	1	2	1	2	M _p ^d	M _n ^e	D ^f	M _p ^d	M _n ^e	D ^f
poly-1 _{TMC10}	TMC		10		10.3		1.2	1.1	2.4	20.2	8.4	2.7
poly-2 _{CL5}	ε-CL		5		6.9		1.8	2.0	1.6	14.8	3.9	3.4
poly-2 _{CL10}	ε-CL		10		11.7		2.9	3.5	1.2	42.8	9.0	4.8
poly-2 _{CL20}	ε-CL		20		25.6		9.4	5.1	1.4	25.5	11.0	2.5
poly-3 _{LA20}	DL-lactide ^g		10		21.1		1.5	1.1	2.0	8.7	1.5	4.1
poly-4 _{TMC5/CL5}	TMC	ε-CL	5	5	6.0	5.3	3.7	2.0	2.1	16.5	7.7	2.3
poly-5 _{GA10/CL5}	glycolide ^g	ε-CL	5	5	6.8	5.0	3.0	1.8	1.8	38.7	7.7	4.6

^aThe polymers are labeled with a number [identical numbers identify polymers synthesized from the same (set of) monomers] followed by the type of monomer and expected average number of monomer units per oligomer repeat unit. ^bMonomer feed (equiv) with respect to 1 equiv of azobenzene initiator **1**. ^cAverage number of monomer units per oligomer repeat unit (¹H NMR). ^dMolar mass of the highest intensity (SEC). ^eNumber-average molar mass (kg/mol) (SEC). ^fPolydispersity index (SEC). ^gOne monomer results in two monomer units.

Scheme 2b,c) provide evidence for the formation of poly-1_{TMC10}. Additionally, the ¹H diffusion-ordered spectroscopy (DOSY) NMR spectrum of poly-1_{TMC10} was acquired to provide further evidence of the covalent bonds formed between individual oligomers (cf. Scheme 2d). Herein, the ¹H NMR signals (horizontal axis) are resolved with respect to their diffusion coefficients (vertical axis). As a consequence, all signals that refer to a single molecule appear on a horizontal line and are separated from other molecules' signals that have a different diffusion behavior. The signals of acetal, azobenzene, and TMC moieties are horizontally aligned; thus, they share the same diffusion coefficient, proving their incorporation into a single polymer chain. In this way, this two-step one-pot procedure afforded the desired main-chain-functionalized polymer poly-1_{TMC10}, in which the azobenzene units are separated by blocks with an average degree of polymerization of 10 units of TCM.

This easy synthetic strategy can be extended also to the preparation of different main-chain-functionalized polymers, for example, by changing the average distance between the chromophores (by changing the monomer-to-initiator ratio) and the type of oligomers (by changing the monomer), providing an efficient tool for the preparation of a wide range of polymers containing photoswitches in their main-chain. To demonstrate this versatility, other polymers have been prepared from different monomers and different feed ratios with respect to the initiator **1**. For all one-pot syntheses, the molar masses of the synthesized oligomers (first step) and polymers (second step) are listed in Table 1.

First, the lactones ε-caprolactone (ε-CL) and DL-lactide as commercially relevant monomers⁴¹ were used instead of the carbonate TMC. Both monomers (in a 10-fold excess to initiator **1**) were successfully converted into the respective polymers poly-2_{CL10} and poly-3_{LA20}, respectively. Note that one monomer of DL-lactide yields two lactic acid (LA) units after ROP, hence, the nomenclature LA20. The SGP is again evidenced by the disappearance of vinyl ether signals, the

appearance of acetal signals, and an increase in the molar mass as best seen in the increase of the SEC's peak maximum M_p.⁴²

Next, the feed composition of ε-CL to initiator **1** was altered (5:1 vs 10:1 vs 20:1) to change the average intrachain spacing of azobenzene groups in the final polymers (poly-2_{CL5}, poly-2_{CL10}, and poly-2_{CL20}). The ratios of ε-CL to azobenzene units X in the final polymers were quantified by ¹H NMR (cf. Table 1). The obtained ratios of 6.9, 11.7, and 25.6 show that they are controllable simply by adjusting the feed composition, although slightly higher ratios were observed in the polymers than expected by the feed composition. The average intrachain distance of azobenzene units is, thus, controllable by the applied feed composition.

Finally, we extended the procedure to mixtures of two different monomers in the feed to obtain copolymers. On the one hand, a mixture of TMC and ε-CL was used to produce poly-4_{TMC5/CL5}, a polymer with ester and carbonate groups in the same backbone. The equal monomer feed is reflected in the observed ratio of TMC (6.0) to ε-CL (5.3) units in poly-4_{TMC5/CL5}. On the other hand, the copolymerization strategy can be useful also for the insertion of monomers more difficult to be polymerized. As an example, ε-CL was mixed with glycolide to obtain poly-5_{GA10/CL5} [one glycolide yields two glycolic acid (GA) units after ROP]. Compared to the homopolymer poly glycolic acid (PGA), which is mostly insoluble (aside from fluorinated solvents),⁴³ poly-5_{GA10/CL5} is better soluble in organic solvents such as chloroform and dimethylformamide. A lower ratio of GA (6.8) units in the polymer (as compared to the feed composition) is explained by the incomplete conversion of glycolide, in agreement to previous reports.⁴⁴ Compared to these reports, we observed a higher glycolide conversion of 68% (compared to 34%)⁴⁴ using the catalyst TBD, which we attribute to the effect of ε-CL in the copolymerization that prevents the depolymerization of GA units at the chain end and, thus, shifts the equilibrium toward glycolide polymerization.⁴⁵ The successful introduction of two monomers into a copolymer enables further control of the polymer properties, which are explored next.

2.2. Thermal Properties of the Polymers. The thermal properties of the synthesized polymers were analyzed by differential scanning calorimetry (DSC) and thermogravimetric analysis (TGA). Figure 1 shows the DSC traces of the

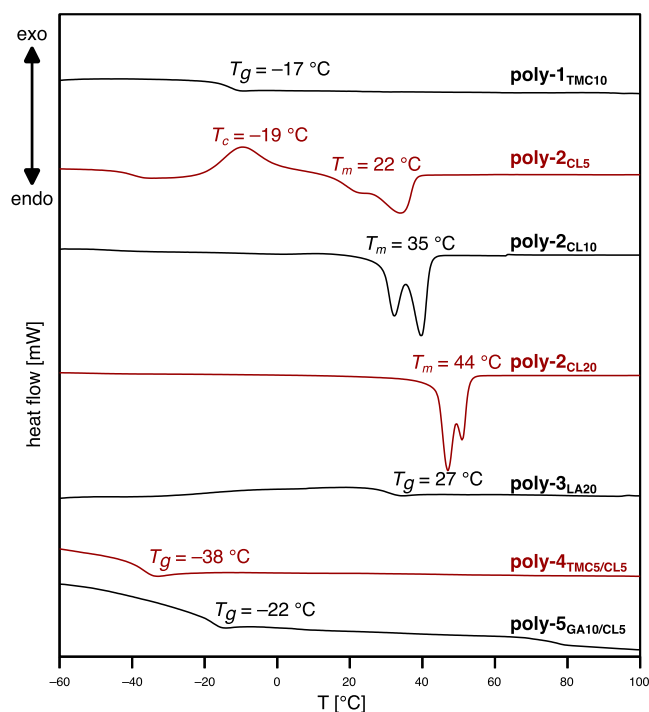


Figure 1. DSC curves of the second heating (10 °C/min). Polymers **poly-2** are semicrystalline and melt upon heating (melting temperature: T_m). **Poly-2_{CL5}** crystallizes during the heating cycle (cold crystallization temperature: T_c), whereas **poly-2_{CL10}** and **poly-2_{CL20}** already crystallized during the preceding cooling cycle (not shown). The other polymers are amorphous and undergo a glass transition (glass-transition temperature: T_g).

second heating cycle for all of the polymers. In Table 2, the thermal properties for the synthesized polymers are listed together with the thermal properties of their respective parent polymers, as reported by others (references are given in the table directly).

All the ϵ -CL homopolymers (**poly-2**) are semicrystalline. Two melting peaks are observed that are indicative of the simultaneous presence of two crystalline structures in the polymers, in agreement with reports of once-folded and extended-chain crystals present in the parent PCL.⁵³ The melting temperature T_m increases with increasing ϵ -CL content but remains lower than the T_m of parent PCL. This observation is rationalized by the different length of ϵ -CL oligomers, which directly dictates the T_m of **poly-2**.⁵⁴ In other words, the longer the ϵ -CL segments, the better **poly-2** resembles parent PCL. Furthermore, longer ϵ -CL segments promote the crystallization of **poly-2** expressed in higher degrees of crystallinity χ_c and higher crystallization temperatures T_c . For **poly-2_{CL5}** (shortest segments of ϵ -CL units), the tendency to crystallize is significantly reduced and comparable to the slow crystallization reported for oligomeric PCL,⁵⁰ which leads to an observed exothermic crystallization peak in the DSC's second heating cycle (cf. **poly-2_{CL5}** in Figure 1). On the other end, **poly-2_{CL20}** (longest segments of ϵ -CL units) has similar a T_c and χ_c as parent PCL, and also its thermal stability $T_{5\%}$ (temperature at which the sample lost 5% of its original mass) is similar. Whether the lower thermal stability of **poly-2_{CL5}** and **poly-2_{CL10}** is a consequence of the segment, length of ϵ -CL units or the molar mass distribution of the whole polymer cannot be deciphered. These results confirm that the intrachain distance of azobenzene units in **poly-2** directly affects the thermal properties of the obtained polymers and that its control through the feed composition enables rational tuning of these properties.

All the other polymers were found to be amorphous, which is expected for polymers based on TMC and DL-lactide as their parent polymers PTMC and PDLLA are also amorphous. The absence of a T_m for **poly-5_{GA10/CL5}**—despite both parent polymers PCL and PGA are semicrystalline—is explained by an interference of both monomer units to form crystalline domains due to their statistical incorporation.⁴³ The glass-transition temperature T_g of **poly-1_{TMC10}** is similar to the parent PTMC. For **poly-3_{LA20}**, on the other hand, a 30 °C lower T_g (as compared to parent PDLLA) is observed and explained by the known influence of the chain length on the T_g for PDLLA.⁵⁵ **Poly-4_{TMC5/CL5}** and **poly-5_{GA10/CL5}** have a T_g in

Table 2. Comparison of the Thermal Properties between the Synthesized Polymers and Their Respective Parent Polymers (Values Taken from the Literature in Bold)

polymer	T_m^a [°C]	$1^{st} \chi_c^b$ [%]	$2^{nd} \chi_c^b$ [%]	T_g^c [°C]	$T_{5\%}^d$ [°C]	T_c^e [°C]
poly-1_{TMC10}				-17	243	
PTMC				-15 ⁴⁶	260 ⁴⁷	
poly-2_{CL5}	22	41.6	31.9		302	-19 ^f
poly-2_{CL10}	35	48.9	42.5		327	7
poly-2_{CL20}	44	65.0	49.9		351	26
PCL	60 ⁴⁸		49 ⁶	-60 ⁴⁸	360 ⁴⁹	30 ⁵⁰
poly-3_{LA20}				27	264	
PDLLA				57 ⁴⁸	400 ⁵¹	
poly-4_{TMC5/CL5}				-38	255	
poly-5_{GA10/CL5}				-22	296	
PGA	225 ⁴⁸			35 ⁴⁸	255 ⁴⁴	

^aMelting temperature (as observed in the second heating cycle). ^bDegree of crystallinity referenced to an infinitely large PCL crystal⁵² [as observed in the first (1st) and second (2nd) heating cycle]. ^cGlass-transition temperature (as observed in the second heating cycle). ^dThermal stability, given as onset temperature of mass loss >5% sample mass. ^eCrystallization temperature as observed in the cooling cycle. ^fCold crystallization was observed in the heating cycle.

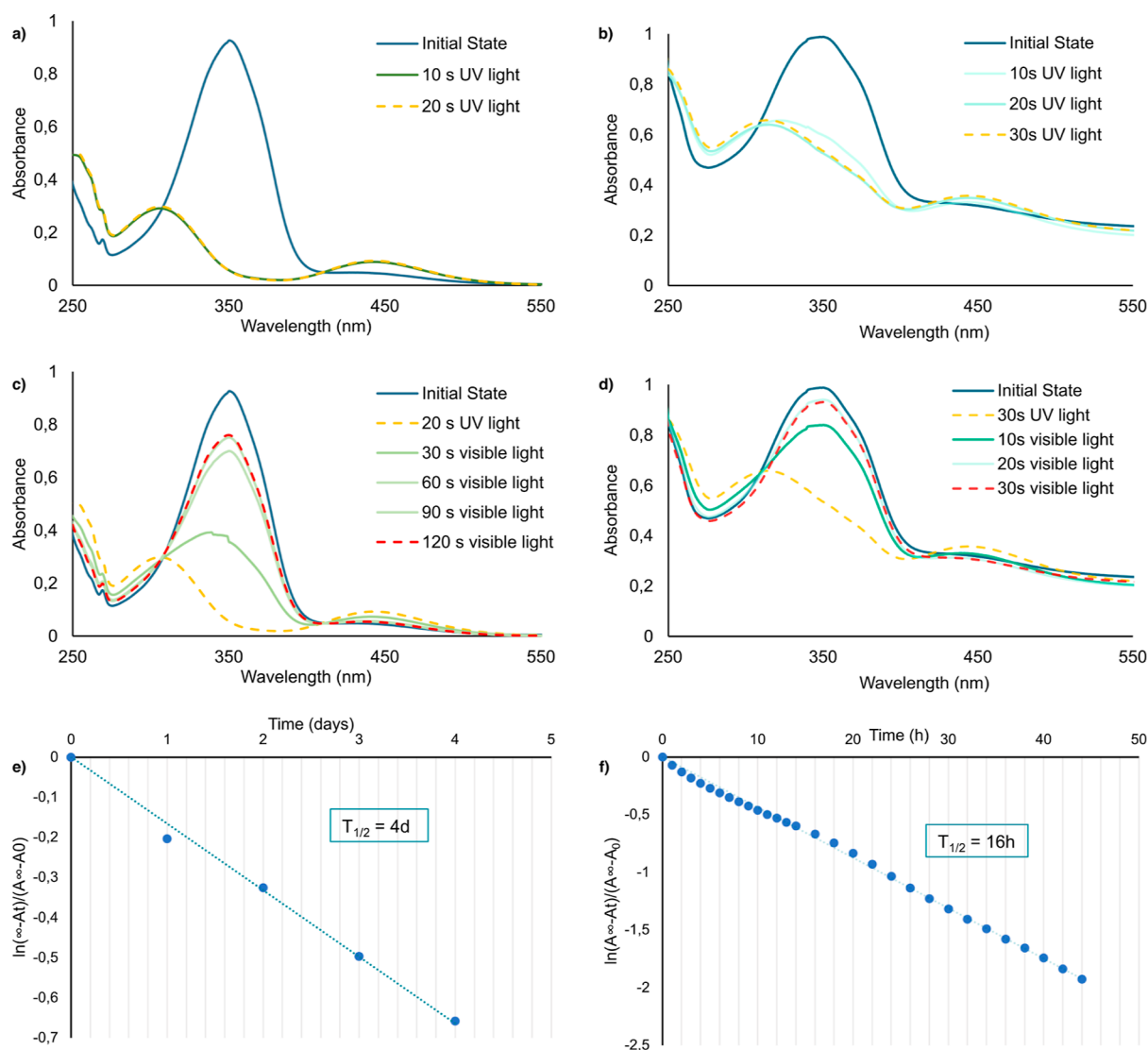


Figure 2. Light-induced isomerization and thermal relaxation processes of the photoresponsive polymer **poly-2_{CL10}** in solution and solid state: (a) solution absorption spectra after UV light irradiation at different times (0 s = initial state); (b) thin-film absorption spectra after UV light irradiation at different times (0 s = initial state); (c) solution absorption spectra after visible light irradiation at different times (0 s = *cis*-pss); (d) thin-film absorption spectra after visible light irradiation at different times (0 s = *cis*-pss); and (e,f) time vs $\ln[(A_{\infty} - A_t)/(A_{\infty} - A_0)]$ plots of the solution (e) and thin film (f) in the dark to calculate the half-life time of the *cis*-isomers for polymers, using the relations of the rate constant k and half-life $t_{1/2}$ of eqs SI-1 and SI-2 (cf. Supporting Information, p. SI-4).

between the T_g of their parent polymers, which is expected for random copolymers.

Incorporation of azobenzene units into the main-chain negligibly affects the thermal stability of **poly-1_{TMC10}**, and the $T_{5\%}$ is only slightly reduced by 17 °C compared to parent PTMC. The thermal stability of **poly-3_{LA20}**, on the other hand, is significantly lower (264 °C) compared to parent PDLA with an $T_{5\%}$ of 400 °C, which we trace back to the relatively low molar mass of **poly-3_{LA20}** compared to the other synthesized main-chain azobenzene polymers. For the copolymers, the thermal stability of **poly-4_{TMC5/CL5}** is similar to its lesser stable parent polymer PTMC, whereas the thermal stability of **poly-5_{GA10/CL5}** is increased by 41 °C (compared to the lesser stable parent polymer PGA) due to the incorporation of the more stable ϵ -CL units. A similar stabilization effect was reported for PGA block copolymers.⁴⁴

2.3. Photochromism in Solution and Solid Thin Films.

The spectroscopic properties of the polymers were studied in

the UV and visible (vis) light regions by UV–vis absorption spectroscopy. Spectra of the dissolved and neat (film) polymers were measured in their initial state (before irradiation), after exposure to UV light (365 nm), and after exposure to visible light (505 nm), whereby the samples were irradiated with light-emitting diodes (LEDs) for selected times. For all the polymers, the spectroscopic behavior is similar and comparable to unsubstituted azobenzene.³³ The initial states are predominantly composed of the thermally stable *trans*-azobenzenes, irradiation with UV light leads to *cis*-enriched states, and visible light irradiation restores *trans*-enriched states. An example of the different experiments performed is reported for **poly-2_{CL10}** in Figure 2. The spectra for the other polymers are reported in the Supporting Information (cf. Figures SI-2–SI-15).

The absorption spectrum of the polymer containing mainly the azobenzene *trans*-isomer was characterized by two absorption bands: the first one, with a higher absorption

intensity, has a maximum around 350 nm and corresponds to the π - π^* transition, whereas the second band, with a maximum around 443 nm, indicates a π - n^* transition.

In analogy with other azobenzene polymers, during UV light (365 nm) irradiation,^{56,57} a photoinduced *trans*-*cis* isomerization occurs and is detected by variation of the absorption spectrum, as shown in Figure 2a. In particular, the absorbance decreased in the first band and increased in the second one. Irradiation of the diluted solution for 10 s was sufficient to obtain the pss, characterized by an absorbance that does not change upon further UV-light irradiation and the presence of the *cis*-isomer as prevalent species. From the absorbance differences at the peak maximum (350 nm), the ratio of *trans*-isomers was approximated under the assumptions of (i) Beer-Lambert's law and (ii) reference absorbance spectra of poly-2_{CL10} in solution for which the *trans*-isomer ratio was independently determined by ¹H NMR analysis (cf. Supporting Information on p. SI-43f. for further details and tabulated values). Based on these assumptions, the achieved *trans*/*cis*-conversion was quantified to be 70–80% for all polymers in solution upon UV-light exposure. Other commercially available LEDs (340 and 385 nm) were also used to irradiate the polymer poly-2_{CL5}, as shown in Figure SI-16. However, the pss produced by these LEDs had a lower quantity of *cis*-isomer than the one obtained by 365 nm irradiation. Although the ideal wavelength can only be identified with monochromatic laser experiments and visualized by the respective action plots,⁵⁸ we selected the 365 nm LED for the remainder of the study.

The process was reversed by irradiation with visible light (505 nm), as shown in Figure 2b. The spectra were taken after 90 and 120 s of irradiation overlap, but the initial state is not fully recovered, indicating that the reached pss has a lower *trans*-isomer ratio compared to the initial state (before irradiation). We quantified the *trans*-isomer ratio of this pss to be approximately 10% points lower as compared to the initial state. However, the photoisomerization processes are entirely reversible in the subsequent cycles (cf. Supporting Information, Figures SI-2–SI-8), which indicates that the difference between the initial state and pss is not caused by photodegradation.

By preparation of a thin film, the spectroscopic properties of all polymers in their solid state were investigated next. Again, the spectra of poly-2_{CL10} are shown in Figure 2b,c, the spectra of the other polymers are reported in the Supporting Information (Figures SI-9–SI-15). Compared to the measurements of the polymer solutions, the absorbance does not reach zero above 550 nm because of scattering effects, which could be treated by a baseline correction (cf. Supporting Information, p. 43f.).⁵⁹ Furthermore, the time required until the polymer films reached their pss by UV irradiation was longer and ranged from 10 to 70 s (30 s in Figure 2b). This difference in irradiation time is likely caused by the optical denser films that lead to a less effective light penetration into the material and a decreased molecular mobility in the solid state (as compared to the solutions), combined with a variation in film thickness (among the polymer films). Due to the same reasons, the *cis*-isomer ratio in the reached pss was lower as compared to the pss of the polymer solution. On the contrary, the return to the *trans*-enriched pss upon irradiation with visible light occurs faster than that in solution (30 s for the film vs 90 s for the solution). We exclude that the faster photoisomerization of the films to the *trans*-isomers is due to a thermal degradation of the

samples since, as Figure SI-17 illustrates, thermal camera images show that green light irradiation does not lead to a practically significant temperature change on the irradiated polymer surface ($\Delta T < 1$ °C). Instead, the faster isomerization with visible light as compared to isomerization with UV light could be explained by the lower optical density of the sample in the visible region (as compared to the UV region), which improves the light penetration. The faster *cis*-isomerization of the solid films as compared to the dissolved polymer could partly be explained by the lower *cis*-isomer ratio of the films (compared to the solutions). Furthermore, this faster isomerization to the *trans*-isomers could indicate that the half-life of the *cis*-isomer kept in the dark is lower in the solid state, which is explored in the next paragraph.

To elucidate and compare the stability of the *cis*-isomers between solution and solid film, their thermal stability and their spontaneous thermal relaxation back to the *trans*-isomers at room temperature in the absence of any light source were next investigated. Therefore, after reaching the *cis*-isomer pss by UV irradiation, the samples were kept in the dark, and their absorbance were monitored at predefined time intervals (cf. Figure 2e,f). Assuming that the process follows first-order kinetics, the characteristic half-life time ($t_{1/2}$) of the *cis*-isomers of every sample was calculated (cf. Supporting Information, p. SI-43 for further details). In solution, the half-lives of the *cis*-isomers found are similar (multiple days to 1 week) and, in general, higher than that in the solid films. For example, the half-life of the *cis*-isomers of poly-4_{TMC5/CL5} shortens from 155 h in solution to 44 h in the solid film. Our findings provide hints of a potentially lower energy barrier for *cis*-to-*trans* isomerization in the solid state compared to solutions; even if this phenomenon has been described previously, its rationalization is still ongoing.^{38,60} The observed kinetics of the thermal relaxation (in the dark) appears to be independent of the azobenzene/dye quantity, crystallinity degree, or glass-transition temperature (T_g) of the polymers, implying a nuanced interplay of factors. This observation confirms previous studies (even if mainly devoted to side-chain polymers) where a clear relationship of the *cis*-stability to the polymer's crystallinity and glass transition was unobserved.^{61–64} Also in our case, there appears to be no obvious relationship between the thermal properties of the polymers and their *cis*-isomer's half-life time in the solid film. Therefore, the *cis*-isomer stability appears to be related to a set of properties unique to each compound, which are of interest to be studied in the near future.

3. CONCLUSIONS

An azobenzene with complementary vinyl ether and alcohol end groups has been synthesized and used as the initiator for the two-step one-pot synthesis of functionalized polymers with multiple azobenzene groups in the polymer's main-chain. The approach is highly flexible as it allows the polymerization of commercially available monomers—traditionally used for ROP—starting from the same azobenzene as the initiator. Consequently, this method is advantageous compared with previous strategies relying on the synthesis of customized functional monomers that constitute the azobenzene moiety. The approach enables convenient and precise control of the obtained microstructure by adjusting the feed composition to fine-tune the polymer properties. We think that our approach can further be used to build even more complex structures, including the copolymerization of different macro-monomers

in the second step or the synthesis of block copolymers in the first step.

The thermal properties of the obtained polymers were rationalized by using the properties of the parent polymers and the peculiarities that arise from the segmented structure of the azobenzene-containing polymers. The control of such properties, together with the azobenzene's ability to photoisomerize both in solution and in neat films, enables the rational design of these and similar polymers for specific applications. Future investigations will focus on the impact of the photoisomerization on the polymer properties and use the polymerization strategy as the platform to develop polymers with stimuli-responsive moieties in their main-chain.

■ ASSOCIATED CONTENT

SI Supporting Information

The Supporting Information is available free of charge at <https://pubs.acs.org/doi/10.1021/acsapm.3c02849>.

Synthesis of the initiator and polymers, including their characterization via NMR, IR, SEC, DSC, and TGA, and UV-vis spectra of the polymers in solution and solid state (PDF)

■ AUTHOR INFORMATION

Corresponding Authors

Daniele Martella – European Laboratory for Non-linear Spectroscopy (LENS), Sesto Fiorentino IT-50019, Italy; Department of Chemistry “Ugo Schiff”, University of Florence, Sesto Fiorentino IT-50019, Italy; orcid.org/0000-0002-8845-0908; Email: martella@lens.unifi.it

Max Hirschmann – Department of Fibre and Polymer Technology, KTH Royal Institute of Technology, Stockholm SE-10044, Sweden; Present Address: Uppsala University, Department of Chemistry—Ångström Laboratory, SE-752 37 Uppsala, Sweden; orcid.org/0000-0003-3276-8076; Email: max.hirschmann@kemi.uu.se

Authors

Ruggero Rossi – European Laboratory for Non-linear Spectroscopy (LENS), Sesto Fiorentino IT-50019, Italy; orcid.org/0009-0006-6674-3319

Camilla Parmeggiani – European Laboratory for Non-linear Spectroscopy (LENS), Sesto Fiorentino IT-50019, Italy; Department of Chemistry “Ugo Schiff”, University of Florence, Sesto Fiorentino IT-50019, Italy; orcid.org/0000-0002-1443-1878

Tiziana Fuoco – Department of Fibre and Polymer Technology, KTH Royal Institute of Technology, Stockholm SE-10044, Sweden; orcid.org/0000-0001-7135-9158

Complete contact information is available at: <https://pubs.acs.org/doi/10.1021/acsapm.3c02849>

Notes

The authors declare no competing financial interest.

■ ACKNOWLEDGMENTS

R.R. and C.P. acknowledge Regione Toscana, Bando Ricerca Salute 2018, PERCARE project for the financial support. R.R. and C.P. also thank MIUR-Italy (“Progetto Dipartimenti di Eccellenza 2018–2022”) for the funds allocated to the Department of Chemistry “Ugo Schiff”. T.F. and M.H. acknowledge Formas—a Swedish Research Council for

Sustainable Development (Early career Researchers grant no. 2020-00910) and Swedish Research Grant (VR, Starting grant no. 2020-03247) for the financial support.

■ REFERENCES

- (1) Yang, C.; Wu, K. B.; Deng, Y.; Yuan, J.; Niu, J. Geared Toward Applications: A Perspective on Functional Sequence-Controlled Polymers. *ACS Macro Lett.* **2021**, *10*, 243–257.
- (2) Deacy, A. C.; Gregory, G. L.; Sulley, G. S.; Chen, T. T. D.; Williams, C. K. Sequence Control from Mixtures: Switchable Polymerization Catalysis and Future Materials Applications. *J. Am. Chem. Soc.* **2021**, *143*, 10021–10040.
- (3) Abdollahi, A.; Roghani-Mamaqani, H.; Razavi, B. Stimuli-chromism of photoswitches in smart polymers: Recent advances and applications as chemosensors. *Prog. Polym. Sci.* **2019**, *98*, 101149.
- (4) Chen, X.; Michinobu, T. Postpolymerization Modification: A Powerful Tool for the Synthesis and Function Tuning of Stimuli-Responsive Polymers. *Macromol. Chem. Phys.* **2022**, *223*, 2100370.
- (5) Png, Z. M.; Wang, C.-G.; Yeo, J. C. C.; Lee, J. J. C.; Suratman, N. E.; Tan, Y. L.; Liu, H.; Wang, P.; Tan, B. H.; Xu, J. W.; Loh, X. J.; Zhu, Q. Stimuli-responsive structure-property switchable polymer materials. *Mol. Syst. Des. Eng.* **2023**, *8*, 1097–1129.
- (6) Fuoco, T. Degradation in order: simple and versatile one-pot combination of two macromolecular concepts to encode diverse and spatially regulated degradability functions. *Angew. Chem., Int. Ed.* **2021**, *60*, 15482–15489.
- (7) Stuart, M. A. C.; Huck, W. T. S.; Genzer, J.; Müller, M.; Ober, C.; Stamm, M.; Sukhorukov, G. B.; Szleifer, I.; Tsukruk, V. V.; Urban, M.; Winnik, F.; Zauscher, S.; Luzinov, I.; Minko, S. Emerging applications of stimuli-responsive polymer materials. *Nat. Mater.* **2010**, *9*, 101–113.
- (8) Wei, M.; Gao, Y.; Li, X.; Serpe, M. J. Stimuli-responsive polymers and their applications. *Polym. Chem.* **2017**, *8*, 127–143.
- (9) Moulin, E.; Faour, L.; Carmona-Vargas, C. C.; Giuseppone, N. From Molecular Machines to Stimuli-Responsive Materials. *Adv. Mater.* **2020**, *32*, 1906036.
- (10) Wang, L.; Li, Q. Photochromism into Nanosystems: Towards Lighting up the Future Nanoworld. *Chem. Soc. Rev.* **2018**, *47*, 1044–1097.
- (11) Bertrand, O.; Gohy, J.-F. Photo-responsive polymers: synthesis and applications. *Polym. Chem.* **2017**, *8*, 52–73.
- (12) Pijper, D.; Jongejan, M. G. M.; Meetsma, A.; Feringa, B. L. Light-Controlled Supramolecular Helicity of a Liquid Crystalline Phase Using a Helical Polymer Functionalized with a Single Chiroptical Molecular Switch. *J. Am. Chem. Soc.* **2008**, *130*, 4541–4552.
- (13) Hirschmann, M.; Soltwedel, O.; Ritzert, P.; von Klitzing, R.; Thiele, C. M. Light-Controlled Lyotropic Liquid Crystallinity of Polyaspartates Exploited as Photo-Switchable Alignment Medium. *J. Am. Chem. Soc.* **2023**, *145*, 3615–3623.
- (14) Zheng, M.; Yuan, J. Polymeric nanostructures based on azobenzene and their biomedical applications: synthesis, self-assembly and stimuli-responsiveness. *Org. Biomol. Chem.* **2022**, *20*, 749–767.
- (15) Zhou, H.; Xue, C.; Weis, P.; Suzuki, Y.; Huang, S.; Koynov, K.; Auernhammer, G. K.; Berger, R.; Butt, H.-J.; Wu, S. Photoswitching of glass transition temperatures of azobenzene-containing polymers induces reversible solid-to-liquid transitions. *Nat. Chem.* **2017**, *9*, 145–151.
- (16) Shen, D.; Yao, Y.; Zhuang, Q.; Lin, S. Mainchain Alternating Azopolymers with Fast Photo-Induced Reversible Transition Behavior. *Macromolecules* **2021**, *54*, 10040–10048.
- (17) Ikeda, T. Photomodulation of liquid crystal orientations for photonic applications. *J. Mater. Chem.* **2003**, *13*, 2037–2057.
- (18) Yu, H.; Iyoda, T.; Okano, K.; Shishido, A.; Ikeda, T. Photoresponsive Behavior and Photochemical Phase Transition of Amphiphilic Diblock Liquid-Crystalline Copolymer. *Mol. Cryst. Liq. Cryst.* **2005**, *443*, 191–199.

- (19) Boissiere, O.; Han, D.; Tremblay, L.; Zhao, Y. Flower micelles of poly(*N*-isopropylacrylamide) with azobenzene moieties regularly inserted into the main chain. *Soft Matter* **2011**, *7*, 9410–9415.
- (20) Ding, L.; Xu, M.; Wang, J.; Liao, Y.; Qiu, J. Controlled synthesis of azobenzene functionalized homo and copolymers via direct acyclic diene metathesis polymerization. *Polymer* **2014**, *55*, 1681–1687.
- (21) Ding, L.; Li, J.; Li, T.; Zhang, L.; Song, W. Linear, Y-shaped, and H-shaped amphiphilic azobenzene copolymers: Facile synthesis and topological effect on self-assembly and photoresponsive property. *React. Funct. Polym.* **2017**, *121*, 15–22.
- (22) Ding, L.; Li, Y.; Cang, H.; Li, J.; Wang, C.; Song, W. Controlled synthesis of azobenzene-containing block copolymers both in the main- and side-chain from SET-LRP polymers via ADMET polymerization. *Polymer* **2020**, *190*, 122229.
- (23) Thai, L. D.; Guimaraes, T. R.; Spann, S.; Goldmann, A. S.; Golberg, D.; Mutlu, H.; Barner-Kowollik, C. Photoswitchable block copolymers based on main chain α -bisimines. *Polym. Chem.* **2022**, *13*, 5625–5635.
- (24) Bléger, D.; Liebig, T.; Thiermann, R.; Maskos, M.; Rabe, J. P.; Hecht, S. Light-Orchestrated Macromolecular “Accordions”: Reversible Photoinduced Shrinking of Rigid-Rod Polymers. *Angew. Chem., Int. Ed.* **2011**, *50*, 12559–12563.
- (25) Sommer, M.; Komber, H. Spiropyran Main-Chain Conjugated Polymers. *Macromol. Rapid Commun.* **2013**, *34*, 57–62.
- (26) Mineo, P. G.; Rescifina, A.; Abbadessa, A.; Rapisardi, R.; Scamporrino, A. A.; Spitaleri, F. Synthesis and characterization of copolycarbonates having azobenzene units in the main chain as an active group for optical logic gate devices. *Polym. Chem.* **2016**, *7*, 6318–6329.
- (27) Zhong, H.-Y.; Chen, L.; Yang, R.; Meng, Z.-Y.; Ding, X.-M.; Liu, X.-F.; Wang, Y.-Z. Azobenzene-containing liquid crystalline polyester with π - π interactions: diverse thermo- and photo-responsive behaviours. *J. Mater. Chem. C* **2017**, *5*, 3306–3314.
- (28) Paiva, G. M. S.; Duarte, L. G. T. A.; Faleiros, M. M.; Atvars, T. D. Z.; Felisberti, M. I. Z-E isomerization of azobenzene based amphiphilic poly(urethane-urea)s: Influence on the dynamic mechanical properties and the effect of the self-assembly in solution on the isomerization kinetics. *Eur. Polym. J.* **2020**, *127*, 109583.
- (29) Liu, Z.; Yao, Y.; Tao, X.; Wei, J.; Lin, S. Helical Self-Assembly of Amphiphilic Chiral Azobenzene Alternating Copolymers. *ACS Macro Lett.* **2021**, *10*, 1174–1179.
- (30) Ube, T.; Nakayama, R.; Ikeda, T. Photoinduced Motions of Thermoplastic Polyurethanes Containing Azobenzene Moieties in Main Chains. *Macromolecules* **2022**, *55*, 413–420.
- (31) Ma, S.; Wang, L.; Zhou, Y.; Zhang, H. Fully Room Temperature Reprogrammable, Recyclable, and Photomobile Soft Actuators from Physically Cross-Linked Main-Chain Azobenzene Liquid Crystalline Polymers. *Molecules* **2023**, *28*, 4174.
- (32) Pianowski, Z. L. Recent Implementations of Molecular Photoswitches into Smart Materials and Biological Systems. *Chem.—Eur. J.* **2019**, *25*, S128–S144.
- (33) Bandara, H. M. D.; Burdette, S. C. Photoisomerization in Different Classes of Azobenzene. *Chem. Soc. Rev.* **2012**, *41*, 1809–1825.
- (34) Martella, D.; Nocentini, S.; Parmeggiani, C.; Wiersma, D. S. Photonic artificial muscles: from micro robots to tissue engineering. *Faraday Discuss.* **2020**, *223*, 216–232.
- (35) Zong, C.; Hu, M.; Azhar, U.; Chen, X.; Zhang, Y.; Zhang, S.; Lu, C. Smart Copolymer-Functionalized Flexible Surfaces with Photoswitchable Wettability: From Superhydrophobicity with “Rose Petal” Effect to Superhydrophilicity. *ACS Appl. Mater. Interfaces* **2019**, *11*, 25436–25444.
- (36) Rossi, R.; Salvini, A.; Pizzo, B.; Frediani, M.; Wiersma, D. S.; Parmeggiani, C.; Martella, D. Photoresponsive Adhesives Based on Arylazaisoxazoles-Containing Polymers. *Macromol. Mater. Eng.* **2023**, *308*, 2200504.
- (37) Yu, Z.; Hecht, S. Remote Control over Folding by Light. *Chem. Commun.* **2016**, *52*, 6639–6653.
- (38) Eisenbach, C. D. Relation between Photochromism of Chromophores and Free Volume Theory in Bulk Polymers. *Ber. Bunsenges. Phys. Chem.* **1980**, *84*, 680–690.
- (39) Ercole, F.; Davis, T. P.; Evans, R. A. Photo-responsive systems and biomaterials: photochromic polymers, light-triggered self-assembly, surface modification, fluorescence modulation and beyond. *Polym. Chem.* **2010**, *1*, 37–54.
- (40) Wang, S.; Liu, Q.; Li, L.; Urban, M. W. Recent Advances in Stimuli-Responsive Commodity Polymers. *Macromol. Rapid Commun.* **2021**, *42*, 2100054.
- (41) Yu, J.; Xu, S.; Liu, B.; Wang, H.; Qiao, F.; Ren, X.; Wei, Q. PLA Bioplastic production: From monomer to the polymer. *Eur. Polym. J.* **2023**, *193*, 112076.
- (42) Step-growth polymerizations usually lead to a broader molar mass distribution (higher D value) as compared to chain-growth polymerizations (a category that includes the ring-opening polymerization used in the first step). The increased molar mass of the polymers (as compared to the oligomers) is, thus, best seen in the increase of M_p .
- (43) *Handbook of Biodegradable Polymers Synthesis, Characterization, and Applications*; Lendlein, A., Sisson, A. L., Eds.; Wiley-VCH, 2011.
- (44) Kemo, V. M.; Schmidt, C.; Zhang, Y.; Beuermann, S. Low Temperature Ring-Opening Polymerization of Diglycolide Using Organocatalysts with PEG as Macroinitiator. *Macromol. Chem. Phys.* **2016**, *217*, 842–849.
- (45) Cederholm, L.; Olsén, P.; Hakkarainen, M.; Odelius, K. Turning natural δ -lactones to thermodynamically stable polymers with triggered recyclability. *Polym. Chem.* **2020**, *11*, 4883–4894.
- (46) Li, Z.; Mogensen, R.; Mindemark, J.; Bowden, T.; Brandell, D.; Tominaga, Y. Ion-Conductive and Thermal Properties of a Synergistic Poly(ethylene carbonate)/Poly(trimethylene carbonate) Blend Electrolyte. *Macromol. Rapid Commun.* **2018**, *39*, 1800146.
- (47) Sun, B.; Mindemark, J.; Edström, K.; Brandell, D. Polycarbonate-based solid polymer electrolytes for Li-ion batteries. *Solid State Ionics* **2014**, *262*, 738–742.
- (48) *Handbook of Biodegradable Polymers*; Domb, J. K., Abraham, J., Wiseman, D., Eds.; CRC Press, 1998.
- (49) Vogel, C.; Siesler, H. W. Thermal Degradation of Poly(ϵ -caprolactone), Poly(L-lactic acid) and their Blends with Poly(3-hydroxybutyrate) Studied by TGA/FT-IR Spectroscopy. *Macromol. Symp.* **2008**, *265*, 183–194.
- (50) Fernández-Tena, A.; Pérez-Camargo, R. A.; Coulembier, O.; Sangroniz, L.; Aranburu, N.; Guerrica-Echevarria, G.; Liu, G.; Wang, D.; Cavallo, D.; Müller, A. J. Effect of Molecular Weight on the Crystallization and Melt Memory of Poly(ϵ -caprolactone) (PCL). *Macromolecules* **2023**, *56*, 4602–4620.
- (51) Wang, S.; Ma, P.; Wang, R.; Wang, S.; Zhang, Y.; Zhang, Y. Mechanical, thermal and degradation properties of poly(*d,l*-lactide)/poly(hydroxybutyrate-co-hydroxyvalerate)/poly(ethylene glycol) blend. *Polym. Degrad. Stab.* **2008**, *93*, 1364–1369.
- (52) Khambatta, F. B.; Warner, F.; Russell, T.; Stein, R. S. Small-angle x-ray and light scattering studies of the morphology of blends of poly(ϵ -caprolactone) with poly(vinyl chloride). *J. Polym. Sci., Polym. Phys. Ed.* **1976**, *14*, 1391–1424.
- (53) Wang, Z.; He, Y.; Müller, A. J. Using PCL oligomers to study the differences in melting behavior between polymers and small molecules crystals. *Polymer* **2023**, *271*, 125783.
- (54) Pérez-Camargo, R. A.; Arandia, I.; Safari, M.; Cavallo, D.; Lotti, N.; Soccio, M.; Müller, A. J. Crystallization of isodimorphic aliphatic random copolyesters: Pseudo-eutectic behavior and double-crystalline materials. *Eur. Polym. J.* **2018**, *101*, 233–247.
- (55) Zhang, R.; Du, F.; Jariyavidyanont, K.; Zhuravlev, E.; Schick, C.; Androsch, R. Glass transition temperature of poly(*d,l*-lactic acid) of different molar mass. *Thermochim. Acta* **2022**, *718*, 179387.
- (56) Xing, T.; Chang, C.-C.; Xu, W. Thermoplastic Azobenzene Polyurethanes with Both Efficient Photomediated Migration and Excellent Mechanical Strength. *ACS Appl. Polym. Mater.* **2023**, *5*, 6212–6221.

(57) Ceamanos, L.; Mulder, D. J.; Kahveci, Z.; López-Valdeolivas, M.; Schenning, A. P. H. J.; Sánchez-Somolinos, C. Photomechanical response under physiological conditions of azobenzene-containing 4D-printed liquid crystal elastomer actuators. *J. Mater. Chem. B* **2023**, *11*, 4083–4094.

(58) Irshadeen, I. M.; Walden, S. L.; Wegener, M.; Truong, V. X.; Frisch, H.; Blinco, J. P.; Barner-Kowollik, C. Action Plots in Action: In-Depth Insights into Photochemical Reactivity. *J. Am. Chem. Soc.* **2021**, *143*, 21113–21126.

(59) Gratzner, W. B.; Holzwarth, G. M.; Doty, P. Polarization of the ultraviolet absorption bands in α -helical polypeptides. *Proc. Natl. Acad. Sci. U.S.A.* **1961**, *47*, 1785–1791.

(60) Matsumoto, M.; Miyazaki, D.; Tanaka, M.; Azumi, R.; Manda, E.; Kondo, Y.; Yoshino, N.; Tachibana, H. Reversible Light-Induced Morphological Change in Langmuir-Blodgett Films. *J. Am. Chem. Soc.* **1998**, *120*, 1479–1484.

(61) Eisenbach, C. D. Effect of polymer matrix on the cis-trans isomerization of azobenzene residues in bulk polymers. *Makromol. Chem.* **1978**, *179*, 2489–2506.

(62) Natansohn, A.; Rochon, P.; Pezolet, M.; Audet, P.; Brown, D.; To, S. Azo Polymers for Reversible Optical Storage. 4. Cooperative Motion of Rigid Groups in Semicrystalline Polymers. *Macromolecules* **1994**, *27*, 2580–2585.

(63) Barrett, C.; Natansohn, A.; Rochon, P. Cis-Trans Thermal Isomerization Rates of Bound and Doped Azobenzenes in a Series of Polymers. *Chem. Mater.* **1995**, *7*, 899–903.

(64) Poutanen, M.; Ikkala, O.; Priimagi, A. Structurally Controlled Dynamics in Azobenzene-Based Supramolecular Self-Assemblies in Solid State. *Macromolecules* **2016**, *49*, 4095–4101.